J Electr Eng Technol Vol. 8, No. 3: 595-602, 2013
http://dx.doi.org/10.5370/JEET.2013.8.3.595

ISSN(Print) 1975-0102
ISSN(Online) 2093-7423

Contact Parameter Computation and Analysis of Air Circuit Breaker with Permanent Magnet Actuator

Shuhua Fang†, Heyun Lin*, S. L. Ho, Xianbing Wang*, Ping Jin*, Yunkai Huang* and Shiyou Yang*****

Abstract – An air circuit breaker (ACB) with novel double-breaker contact and permanent magnet actuator (PMA) is presented. Three-dimensional (3-D) finite element method (FEM) is employed to compute the electro-dynamic repulsion forces, including the Holm force and Lorentz force, which are acting on the static and movable contacts. The electro-dynamic repulsion forces of different contact pieces are computed, illustrating there is an optimal number of contact pieces for the ACB being studied. The electro-dynamic repulsion force of each contact, which varies from the outer position to the inner position, is also computed. Finally, the contacts of the double-breaker are manufactured according to the analyzed results to validate the simulations.

Keywords: Double-breaker contact, Permanent magnet actuator, Air circuit breaker, Electromagnetic repulsion force

1. Introduction

Circuit breaker (CB) is an indispensable element for switching on and off of power supply in a power system. The modern trend is to develop CBs which are compact in size and large in current interrupting capacity. Double-breaker CBs with two breaker contacts can interrupt higher short circuit or fault currents when compared to their single-breaker counterparts of similar size. However it is very difficult to drive the contacts of double-breaker CB using conventional spring actuator (SA). To reduce the size of CBs, permanent magnet actuator (PMA), which is becoming a key constituent of vacuum circuit breakers (VCB), is now being extensively developed [1-5]. As PMA is able to produce greater holding force than SA with the same physical size, PMA is finding increasing applications in the design and development of modern double-breaker CBs. Investigations and studies into the design of double-breaker CB with PMA, which includes the PMA design, PMA optimization, movement simulation [6], PMA control [7], short-time withstand current calculation, contact parameter computation and so on are challenging and topical issues facing the designers.

It is well known that computation of the electro-dynamic repulsion force is the key to optimal design of CBs. Indeed there is a wealth of work being reported on electro-dynamic repulsion force computation. In [8], the short-time withstanding current of a spring operated double-breaker ACB is calculated. Ito and Li report their research on the blowout and electro-dynamic repulsion forces acting on the contacts of molded case circuit breakers [9-10]. Liu uses three-dimensional (3-D) finite element method (FEM) to study the electro-dynamic repulsion force of a single-breaker ACB driven by SA [11]. However, there is no literature that reports the computation of contact dynamics of double-breaker ACB with PMA.

The purpose of this paper is to present a new type of contacts with double-breaker in an ACB driven by PMA. 3-D FEM is employed to compute the electro-dynamic repulsion forces between the static and movable contacts. The electro-dynamic repulsion forces of different pieces of contacts are also computed, and each piece of contact is analyzed in details.

2. Mathematics Model

2.1 Holm force

To analyze the electro-dynamic repulsion force, it is assumed that either there is only one conducting zone, hereinafter referred as the conductive bridge in this paper, or all the conducting zones are focused at the center of the contact as shown in Fig. 1. Fig. 1(a) shows the cross-section of the contacts which include the movable contact, static contact and conductive bridge. Figs. 1(b) and 1(c) illustrate the cylindrical and rectangular contacts. Additionally, to simplify the computation, the conducting zone is considered as an equipotential superconducting ball with a radius r instead of being a plane. With these

† Corresponding Author: School of Electrical Engineering, Southeast University, China.(shfang@seu.edu.cn)
* School of Electrical Engineering, Southeast University, China. (hyling@seu.edu.cn; seueelab_wxb@163.com; seueelab_jp@163.com; huangyk@seu.edu.cn)
** Dept. of Electrical Engineering, Hong Kong Polytechnic University, Hong Kong.(eeslho@polyu.edu.hk)
*** College of Electrical Engineering, Zhejiang University, China. (shiyouyang@yahoo.com)
Received: November 14, 2011; Accepted: October 24, 2012

assumptions, the shrink area is not an ellipsoidal surface but a series of spherical surfaces which are concentric with the superconducting ball, along the radial line in which the currents are flowing. The electro-dynamic repulsion force contributed by the shrink current is referred as the Holm force [12].

$$F_H = \frac{\mu_0}{4\pi} I^2 \ln \frac{R}{r} = \begin{cases} \frac{\mu_0}{4\pi} I^2 \ln\left(\frac{\xi H \pi R^2}{P}\right)^{1/2} \\ \frac{\mu_0}{4\pi} I^2 \ln\left(\frac{\xi HWL}{P}\right)^{1/2} \end{cases} \quad (1)$$

where, I is the current flowing through the contact, R is the contact radius of the cylindrical contact, W and L are the respective width and length of the rectangular contact, r is the radius of the conductive bridge, ξ is the surface conditioning coefficient which varies within the range [0.3-0.6], H is the Brinell hardness, P is the contact force.

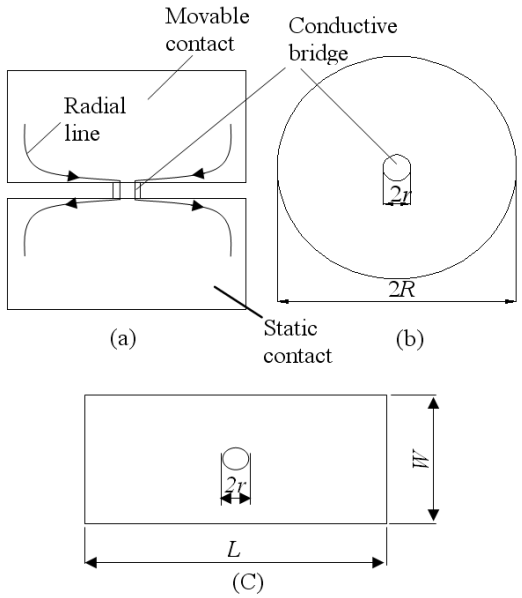

Fig. 1. Contact model, (a) cross-section of the movable contact, static contact and conductive bridge (b) cylindrical contact (c) rectangular contact

2.2 Lorentz force

Since the eddy current has little effect on the electro-dynamic repulsion force, the static electromagnetic field equation can be employed to solve the current density and flux density distributions. The electric vector potential $\boldsymbol{T}$ is used to calculate the current density using

$$\boldsymbol{J} = \nabla \times \boldsymbol{T} \quad (2)$$

where $\boldsymbol{T}$ satisfies the governing equation

$$\nabla \times \left(\frac{1}{\sigma} \nabla \times \boldsymbol{T}\right) = 0 \quad (3)$$

where σ is the electric conductivity. The current constrain condition is

$$\oint_s \boldsymbol{T} \cdot dl = \boldsymbol{I} \quad (4)$$

Once the current density $\boldsymbol{J}$ is obtained, the magnetic vector potential $\boldsymbol{A}$ is employed to decide the flux density $\boldsymbol{B}$

$$\boldsymbol{B} = \nabla \times \boldsymbol{A} \quad (5)$$

In the whole field region, $\boldsymbol{A}$ satisfies the following governing equation:

$$\nabla \times \left(\frac{1}{\mu} \nabla \times \boldsymbol{A}\right) = \boldsymbol{J} \quad (6)$$

where μ is the permeability.

The contact force density f is dependent on the current density and flux density, and the electromagnetic force is calculated by

$$F = \int_V f dV = \int_V \boldsymbol{J} \times \boldsymbol{B} dV \quad (7)$$

where V is the contact volume. Using the conductive bridge model, the Holm force and Lorentz force acting on the contact can be computed using FEM.

3. Computation of the Contact Electro-Dynamic Repulsion Force and Movement Simulation

3.1 The contact system of the ACB with PMA

Fig. 1 shows the proposed contact model for the ACB with PMA. The main mechanical motion system mainly consists of the PMA, a rotating shaft, a cam, insulated plastic, a guide track and a movable contact. When either the making coil or breaking coil of the PMA is excited, the movable iron of the PMA will move up or down to realize the making or breaking operation. The cam is driven by a movable iron, and the rotating shaft transmits the movement of the cam to the insulated plastic in the horizontal direction as shown in Fig. 2. Since the movable contact is latched together with the insulated plastic, it moves along the guide track.

Fig. 3 shows the open and closed positions of the static

contact and movable contact. Fig. 3(a) shows the open position between the static contact and the movable contact. In this CB, the distance d between the static and movable contacts is 22 mm. Fig. 3(b) shows the closed position and depicts the forces acting on the static and movable contacts. When the movable contact realizes the making operation, the current passes through the static and movable contacts as shown by the arrows in Fig. 3. The whole contact system is acted upon by the Holm force, Lorentz force, spring anti-force and thrust force which are generated by the PMA. Additionally, the movable parts are also acted upon by frictional forces as the contact moves.

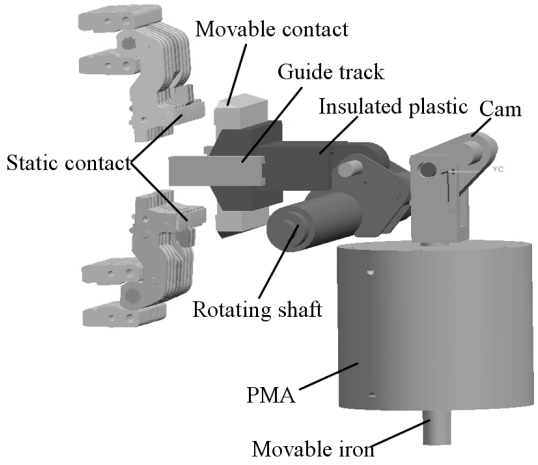

Fig. 2. Assembly of the contact located on the ACB

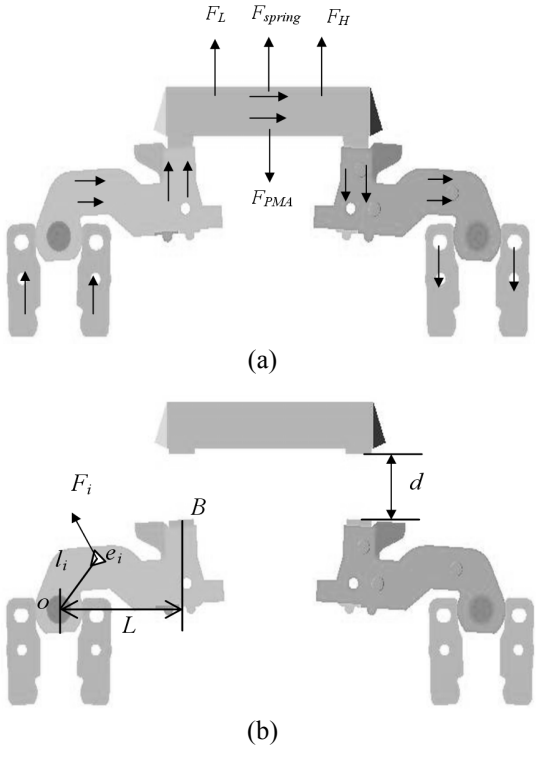

Fig. 3. The static contact and movable contact position: (a) At the open position; (b) At the closed position

For each element e_i as shown in Fig. 3(b), the electro-dynamic repulsion force to the conductive bridge center (point B) can be computed from

$$\boldsymbol{F} = \sum \boldsymbol{F}_i' = \sum \frac{\boldsymbol{F}_i \cdot l_i}{L} \tag{9}$$

where $\boldsymbol{F}_i$ is the electromagnetic force of the static contact element, l_i is the distance between the element center and the rotor axis center (point O), L is the distance between point O and point B and L=50mm, $\boldsymbol{F}_i'$ is the converted electro-dynamic repulsion force of each element between point O and point B.

Fig. 4 shows the three forces acting against permanent magnet force F_{PMA}. Fig. 4(a) are F_{PMA} and the spring force with respect to displacement. Fig. 4(b) presents the variation of the Lorentz force F_L and Holm force F_H acting on phase A as a function of time. In the closed position, the contact system satisfies the following equation:

$$F_{PMA} = F_L + F_H + F_{spring} \tag{8}$$

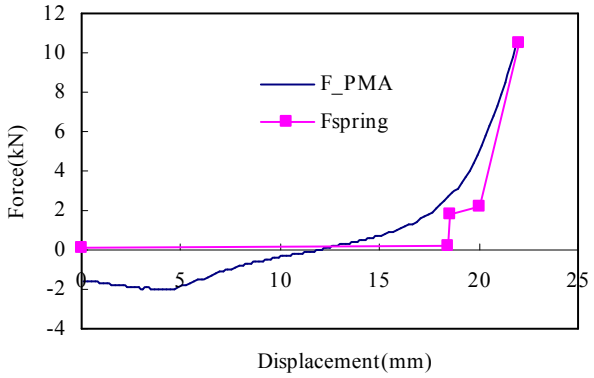

(a)

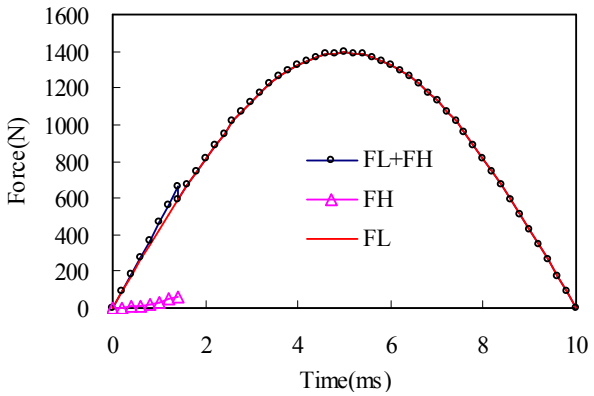

(b)

Fig. 4. Three forces which are, namely F_{spring}, F_L and F_H are acting against permanent magnet force: (a) permanent magnet force F_{PMA} and spring force F_{spring}; (b) Lorentz force F_L and Holm force F_H for the phase A.

3.2 Computation of the contact electro-dynamic repulsion Force

The electro-dynamic force is computed by the conductive bridge model proposed in [9], in which the superconductive balls are substituted by cylindrical elements. The Holm force and Lorentz force acting on the movable contacts are computed by 3-D finite element analysis. The computed model is firstly built in the Unigraphics (UG) software and saved in parasolid format to allow the model to be recognized by the ANSYS finite element software. With this proposed arrangement, the finite element preprocessing time is substantially reduced. The detailed computation flow chart of this algorithm is shown in Fig. 5. In this study the force of one phase with constant direct current is evaluated by solving the current density $\boldsymbol{J}$ of each element with FEM. The $\boldsymbol{J}$ of each element is then loaded in order to compute the magnetic flux density $\boldsymbol{B}$. Once $\boldsymbol{J}$ and $\boldsymbol{B}$ are obtained, the contact force can be computed using Eq. (7).

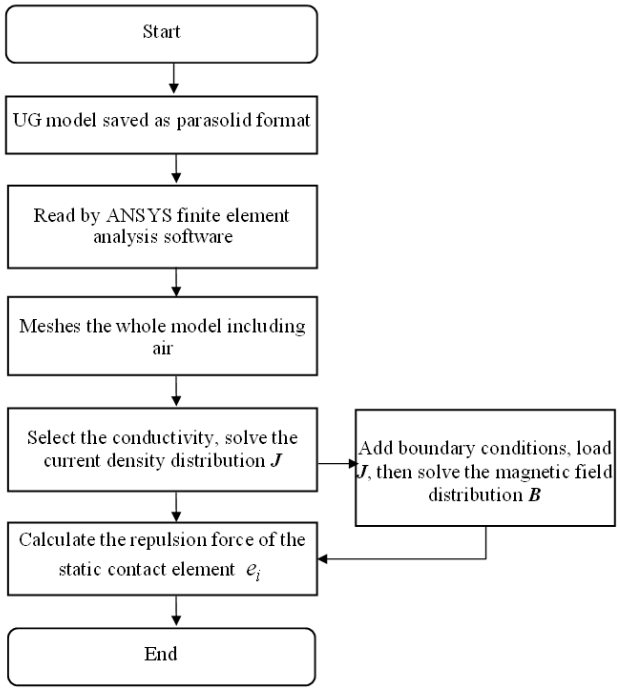

Fig. 5. Computation flow chart

3.3 Movement simulation of the contact

The movement of the contact can be co-simulated in the finite element analysis as well as in the Adams and Matlab software. The magnetic field is computed using FEM to find out the relationship among the flux linkage, displacement and current, and such information is stored in a look-up table. The control model, which is built in Matlab, is connected with the Adams model via input and output interfaces. Detailed movement simulation can be referred to the work of our research group and hence is not repeated here [7]. Fig. 6 shows the result of the movement simulation of the contact.

4. Finite Element Analysis

Since the contacts are symmetrical both on the left and right and they are connected in series, a quarter of the model suffices for the computation of the repulsion force. The analyzed FEM domain is shown in Fig. 7. Two layers of air including Air I and Air II are used to build the model being studied. Air I is fine-meshed, while for the Air II

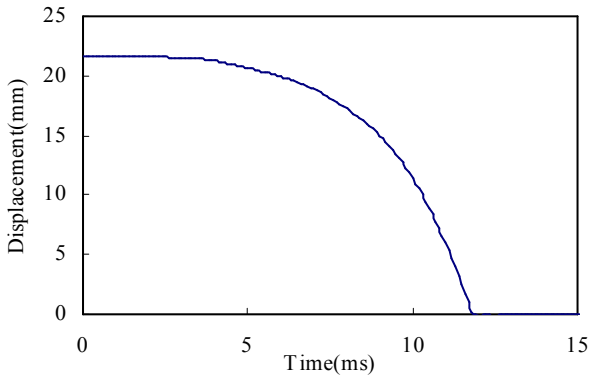

Fig. 6. The movement simulation of the contact

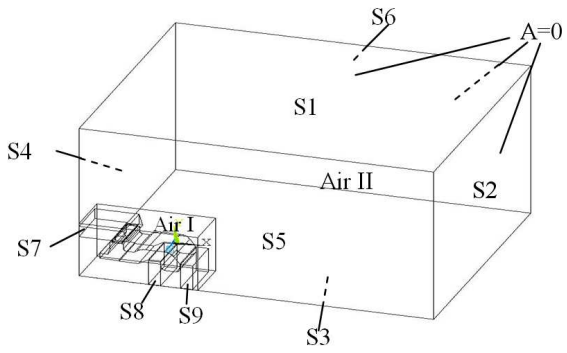

Fig. 7. The analyzed model in ANSYS

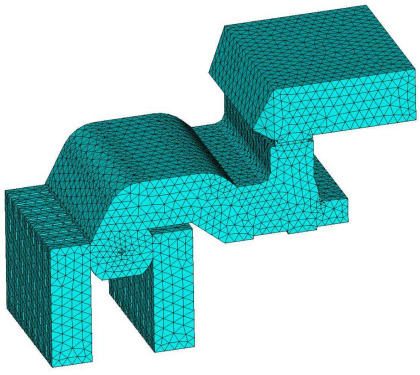

Fig. 8. Meshes of the contact for a quarter of the model

layer, the domain is coarse-meshed to reduce the computing time. The magnetic vector potential $\boldsymbol{A}$ of the boundaries S1, S2 and S6 is set to zero in the ANSYS model. 3-D FEM is employed to analyze the electro-dynamic repulsion force of the contacts. When computing the current density $\boldsymbol{J}$, the freedom of VOLT in ANSYS is coupled to S7, S8 and S9. A node is chosen from S7 and supplied with a current of 50 kA; S8 and S9 are coupled with VOLT=0. Consequently, the current would circulate in the contacts and their corresponding current density $\boldsymbol{J}$ is distributed automatically. Fig. 8 shows the meshes of a quarter of the model for the contacts. The element and node numbers are 46539 and 53925, respectively. Fig. 9 shows the current density distributions, including those in the parallel and single contacts. Since the short circuit current focuses on the conductive bridge between the movable contact and the static one, the maximum magnetic flux density can be above 4T as shown in Fig. 10.

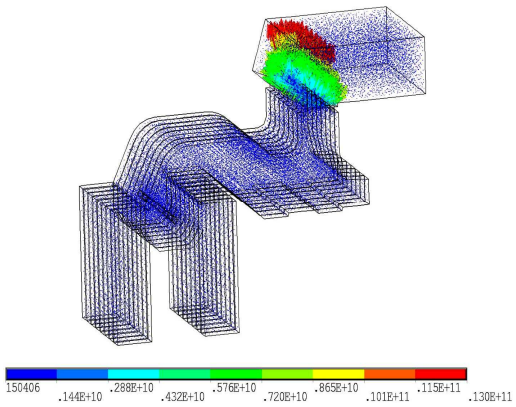

(a)

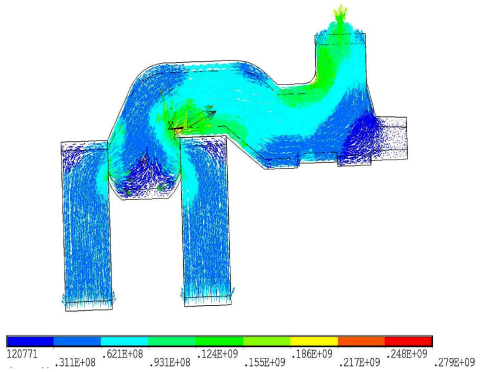

(b)

Fig. 9. Current density distribution (a) Parallel contact (b) Single contact

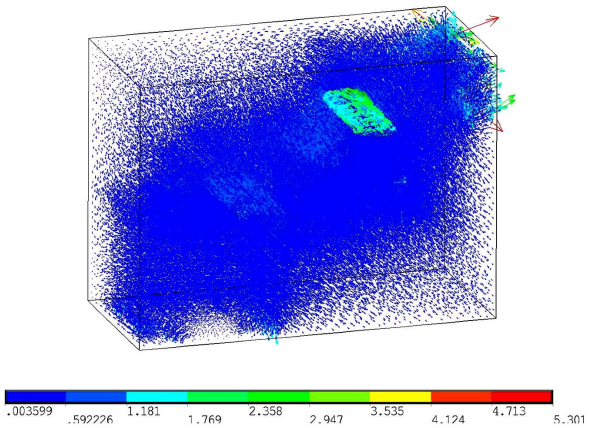

Fig. 10. Magnetic field distribution

5. Contact Parameter Analysis

5.1 The best pieces choice of static contact

Assuming the width (W) of the static contact is constant in the low voltage ACB being designed, one has

$$W = w \cdot N \tag{10}$$

where, w is the width of each piece, N is the number of pieces and W=89.5mm. The electro-dynamic repulsion force for 2 to 20 contact pieces is computed as shown in Fig. 11. It can be seen that the electro-dynamic repulsion force acting on the static contacts decreases as the number of contact piece increases. The figure shows there is an optimal number of contact pieces. If the number of contact pieces is too large, the contact intensity will be weakened. On the other hand, if the number is too small, the electro-dynamic repulsion force will increase substantially. The computed profile also shows that the change from 12 to 20 pieces is not substantial. Thus for the double-breaker CB, the best number of static contact pieces is 16 if both the intensity and electro-dynamic repulsion force are taken into consideration collectively.

5.2 Electromagnetic repulsion force distribution analysis

The paper computes the electro-magnetic repulsion of double-breaker contacts. The computed results are found to concur with those of the single-break circuit breaker proposed in [11]. During the short circuit withstand test, the contacts are supplied with a direct current of 100 kA. Since the contacts are symmetrical on both left and right, the current intensity in the finite element analysis for the quarter model is taken as 50 kA. Fig. 11 depicts the electro-dynamic repulsion force of all the contact pieces. It can be observed that the electro-dynamic repulsion forces increases from the outermost piece (denoted as 1 in Fig.12) to the inner pieces (denoted as 5, 6, 7 and 8 in Fig. 12). The maximum value is larger than the minimum value by about 23.3% and such factor should be taken into consideration when designing the anti-force spring and PMA. The variation of electromagnetic repulsion force coincides with that of single contact circuit breaker, which explains why

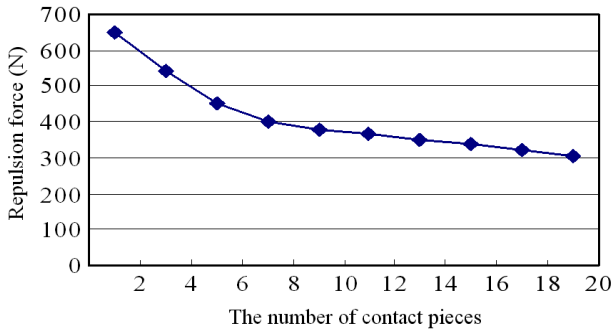

Fig. 11. The electro-dynamic repulsion force for different number of contact pieces with a current i=50kA

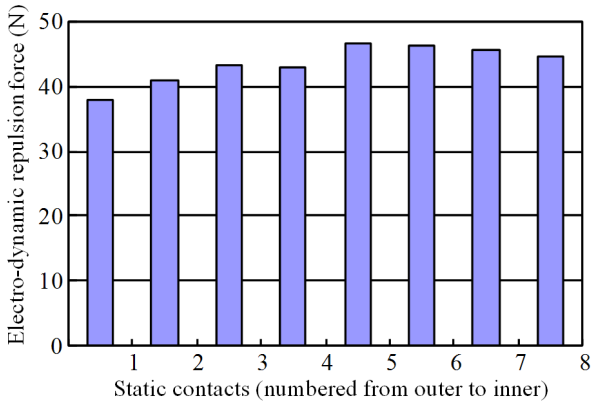

Fig. 12. Electro-dynamic repulsion force distribution of each pieces contact with a current i=50 kA

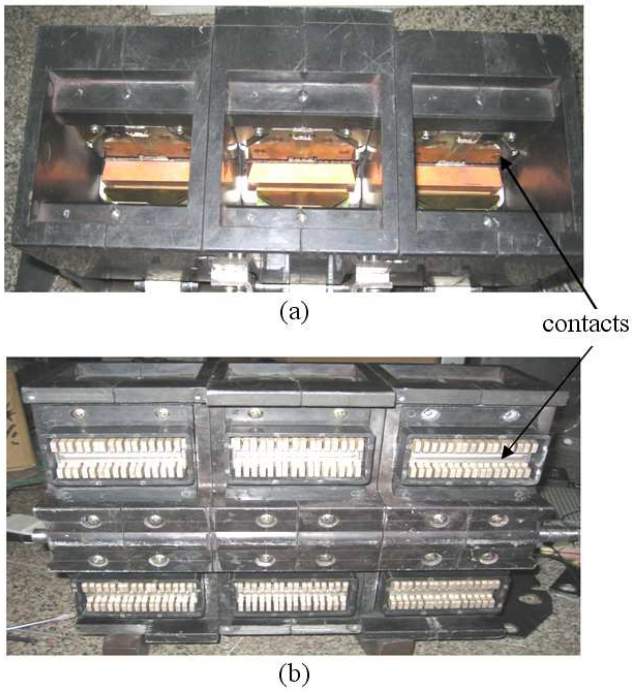

Fig. 13. Prototype and contacts: (a) Top overview; (b) Back overview

the outer contacts are ablated more readily when compared with those in the inner contacts as reported in [11] during the short circuit withstand test. Fig. 13 shows the prototype of a double-breaker contact for the ACB with PMA. The double-breaker contact of ACB driven by PMA is manufactured according to the analyzed results.

6. Conclusion

An air circuit breaker (ACB) with novel double-breaker contact and permanent magnet actuator (PMA) is presented in this paper. 3-D FEM is used to compute the electro-dynamic repulsion forces of double-breaker contact for an ACB with PMA successfully. For the proposed ACB it is found that, within limits, the electro-dynamic repulsion force acting on the static contact decreases as the number of the contact pieces increases. Additionally, it is found that the repulsion forces on the static contacts of the outermost pieces are lower than those in the inner pieces by about 23.3% and this factor must be taken into consideration in the optimal design of the double-breaker contact.

Acknowledgment

This work was jointly supported by the NSFC (50907007), the SRFDP (20090092120041), the NSF of Jiangsu Province (BK2010197), and the Key Projects in the Changzhou Science & Technology Pillar Program (CE20110024).

References

[1] E. Dullni, "A vacuum circuit-breaker with permanent magnetic actuator for frequent operations," in *Proc. XVIIIth Int. Symp. Discharges and Electrical Insulation in Vacuum*, Aug. 1998, Vol. 2, pp. 688-691.

[2] F. G. Liu, H. Y. Guo, Q. X. Yang, L. Zhang and W. L. Yan, "An improved approach to calculate the dynamic characteristics of permanent magnetic actuator of vacuum circuit break," *IEEE Trans. Applied Superconductivity*, Vol. 14, No. 2, pp. 1918-1921, 2004.

[3] S. Nitu, C. Nitu, G. Tuluca, and G. Dumitrescu, "Dynamic behavior of a vacuum circuit breaker mechanism," in *Proc. 23rd Int. Symp. Discharges and Electrical Insulation in Vacuum*, Vol. 1, pp. 181-184, Sept. 2008.

[4] K. I. Woo and B. I. Kwon, "Characteristic analysis and modification of PM-type magnetic circuit breaker," *IEEE Trans. Magn.*, Vol. 40, No. 2, pp. 691-694, March 2004.

[5] S. L. Ho, Y. Li, H. Cui, E. W. C. Lo, S. Y. Yang, H. C. Wong, and K. F. Wong, "Niched genetic simulated

annealing algorithm in the optimization design of a permanent magnetic actuator for a 40.5 kV vacuum circuit breaker," in *Proc. 12th Biennial IEEE Conf. Electromagn. Field Comput.*, Apr. 2006, pp. 410-410.

[6] S. H. Fang, H. Y. Lin, S. L. Ho, X. B. Wang, P. Jin, and H. C. Liu, "Characteristics analysis and simulation of permanent magnet actuator with a new control method for air circuit breaker," *IEEE Trans. Magn.*, Vol. 45, No. 10, pp. 4566-4569, Oct. 2009.

[7] S. H. Fang, H. Y. Lin and S. L. Ho, "Transient co-simulation of low voltage circuit breaker with permanent magnet actuator," *IEEE Trans. Magn.*, Vol. 45, No. 3, pp. 1242-1245, March 2009.

[8] H. G. Xiang, D. G. Chen, X. W. Li, L. Ji, W. X. Tong, "Calculation of the short-time withstand current for air circuit breaker," in *Proc. 53rd IEEE Holm Conf. on Electrical Contacts*, pp. 251-255, 2007.

[9] S. Ito, Y. Takato, Y. Kawase, T. Ota, and H. Mori, "Numerical analysis of electromagnetic forces in low voltage AC circuit breakers using 3-D finite element method taking into account eddy currents," *IEEE Trans. Magn.*, Vol. 34, No. 5, pp. 2597-2600, Sep. 1998.

[10] X. W. Li and D. G. Chen, "3-D finite element analysis and experimental investigation of electrodynamic repulsion force in molded case circuit breakers" *IEEE Trans. Components and Packaging Technologies*, Vol. 28, No. 4, pp. 877-883, Dec. 2005.

[11] Y. Y. Liu, D. G. Chen, X. W. Li, and B. Zhang, "Research on factors affecting electro-dynamic repulsion force in air circuit breaker with the method of 3-D finite element," *Proceedings of the CSEE*, Vol. 25, No. 16, pp. 63-67, 2005.

[12] R. Holm, "Electric Contacts," 4th Ed., Springer-Verlag, 1967.

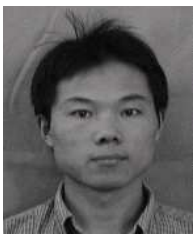

Shuhua Fang He obtained his M. S. degree in electrical engineering from Shandong University of Science and Technology, Jinan, China, in 2004 and his Ph. D. degree in electrical engineering from Southeast University, Nanjing, China, in 2008, respectively.

From 1998 to 2001, he worked as an associate engineer with the Xuzhou Coal and Mine Machinery Factory, where his research activities were primarily in the area of the design, analysis and control of electrical apparatus for coal and mine. Since 2008, he has been with Southeast University, where he is currently an Associate Professor with the School of Electrical Engineering. His research interests include intelligent apparatus design, simulation and control.

Heyun Lin He obtained his B. S., M. S. and Ph. D. degrees in electrical engineering from Nanjing University of Aeronautics and Astronautics, Nanjing, P. R. China, in 1985, 1989 and 1992 respectively. From 1992 to 1994, he worked as a postdoctoral fellow in Southeast University, Nanjing, P. R. China. In 1994, he joined the School of Electrical Engineering, Southeast University as an Associate Professor and is now a Full Professor since 2000. His main research is related to the design, analysis and control of permanent magnet motor, intelligent electrical apparatus and electromagnetic field numerical analysis. He is the author of more than 130 technical papers and holder of 17 patents. Prof. Lin is a member of Electrical Motor and Apparatus Committee of Jiangsu Province, and senior member of both China Society of Electrical Engineering and China Electrotechnical Society.

S. L. Ho He obtained his BSc and Ph. D. degrees in electrical engineering from the University of Warwick, U. K. in 1976 and 1979, respectively. He joined the then Hong Kong Polytechnic in 1979 and is now the Chair Professor and Head of the Department of Electrical Engineering, The Hong Kong Polytechnic University. Since joining the University, Prof. Ho has been working actively with the local industry, particularly in railway engineering. He is the holder of several patents and has published over 250 conference papers and over 240 papers in leading journals, mostly in the IEEE Transactions and IET Proceedings. His main research interests include design optimization of electromagnetic devices, the application of finite elements in electrical machines, phantom loading of machines and railway engineering. Prof. Ho is a member of the Hong Kong Institution of Engineers.

Xianbing Wang He obtained his B. S. degree in electronic information engineering from Beijing University of Technology in 2004. He obtained his M. S. degree in control theory and control engineering from Southwest University of Science and Technology, Mianyang, China, in 2007 and his Ph.D. degree in electrical engineering from Southeast University, Nanjing, China, in 2011, respectively. He joined the Depar-tment of Electronic and Information Engineering, Chuzhou University, Chuzhou, China, in 2011. His research interests include intelligent apparatus design, simulation and control.

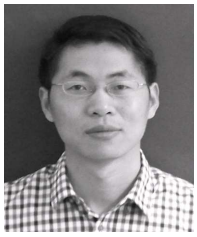

Ping Jin He obtained his B.S. degree in electrical engineering from Nanjing University of Technology in 2004 and his M. S. degree in electrical engineering from the Southeast University, Nanjing, P. R. China in 2008. He is reading for his Ph. D. degree at the Southeast University, Nanjing, P. R. China. From 2004 to 2006, he was an assistant engineer in Jiangsu Construction Engineering Group Corporation Limited to work on civil architectural design and architectural electrical design. His research interests include intelligent apparatus design, simulation and control.

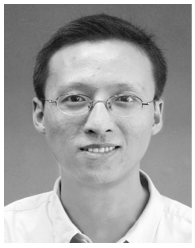

Yunkai Huang He obtained his B. S., M. S. and Ph. D. degrees in electrical engineering from Southeast University, Nanjing, P. R. China, in 1998, 2001 and 2007, respectively. In 2001, he joined the School of Electrical Engineering, Southeast University and is now an Associate Professor since 2008. His main research is related to the design, analysis and control of permanent magnet motor.

Shiyou Yang He received his M.S. degree and Ph.D. degree, both in electrical engineering, from Shenyang University of Technology, in 1990 and 1995, respectively. He is currently a professor of the College of Electrical Engineering, Zhejiang University. His research interests mainly focus on computational electromagnetics.